

DFT Calculations to Study Hydrogen Localization and Diffusion in Disordered Bcc Ti-V-Cr Alloys

O.O. Bavrina^{1,a}, M.G. Shelyapina^{1,b*}, D. Fruchart^{2,c} and N. Novaković^{3,d}

¹Saint Petersburg State University, 7/9 Universitetskaya nab., St. Petersburg 199034, Russia

²Institut Néel CNRS et Université Grenoble Alpes, BP 166, 38042 Grenoble Cedex 9, France

³Vinča Institute of Nuclear Sciences, 12-14 Mike Petrovića Street, Belgrade

^aolga.bavrina@gmail.com, ^bmarina.shelyapina@spbu.ru, ^cdaniel.fruchart@neel.cnrs.fr,
^dnovnik@vinca.rs

Keywords: disordered alloys; metal-hydrogen systems; DFT calculations; hydrogen site solubility; hydrogen diffusion

Abstract. Here we report on the results of our theoretical study of hydrogen localization and motion in disordered bcc Ti-V-Cr alloys. The calculations have been carried out within a DFT supercell approach for a certain composition, namely $\text{Ti}_{0.33}\text{V}_{0.27}\text{Cr}_{0.4}$ for $\text{H}/\text{M} = 1/32$. It was found that hydrogen is localized in highly distorted tetrahedral sites formed by different metal species. H atoms are displaced towards titanium. The estimation of the hydrogen diffusion parameters provides the activation energy value of 0.126 eV and the diffusion coefficient at 294 K equal to $1.9 \times 10^{-10} \text{ m}^2/\text{s}$ that is in good agreement with available experimental data.

Introduction

The hydrogen diffusion in metals attracts much attention from both theoretical and technological point of view, including hydrogen storage in metals, since diffusion, among other, governs hydrogen sorption kinetics. Despite at the beginning of the hydrogen absorption by metals this is the metal surface, on which hydrogen molecules dissociate before penetrating into the bulk, that plays the crucial role, with hydrogen concentration increasing diffusion is the next rate-limiting step in the hydride formation process. Ti-V-Cr alloys with random distribution of metal atoms over the sites of the bcc lattice are considered as promising hydrogen storage materials due to both relatively fast hydrogen sorption kinetics and good hydrogen absorbing capacity, up to 3.7 w% under a few MPa H-gas pressure [1]. Besides, Ti-V-Cr are considered as additives to improve the hydrogen sorption kinetics in the $\text{Mg} \leftrightarrow \text{MgH}_2$ reactions [2]: its bcc structure favors formation of a bcc-Mg structure type at the interface phase boundaries [3]. Moreover, exhibiting rather high hydrogen diffusion coefficient [4], Ti-V-Cr should serve for fast hydrogen delivery to Mg.

Experimental study of hydrogen diffusion in metals can be found in several reports [5–7]. In Ti-V-Cr, hydrogen diffusion is strongly dependent on composition [4,7], especially on the vanadium fraction. Moreover, in Ti-V-Cr alloys with essentially different interactions between hydrogen and metal atoms, the diffusion should be affected by the local structure. To describe hydrogen migration processes at the microscopic level theoretical calculations are highly required.

According to the ternary phase diagram, Ti-V-Cr alloys crystallize mostly into the bcc structure with a random distribution of Ti, V and Cr atoms. In bcc alloys Cr moderates both the stability and the absorption capacity of the corresponding Ti-V-Cr hydrides [8]. At large hydrogen uptakes the hydrides undergo a $\text{bcc} \rightarrow \text{fcc}$ structural phase transformation [8,9]. Recently we proposed a stepwise theoretical approach to study hydrogen diffusion in an fcc-hydride $\text{Ti}_{0.33}\text{V}_{0.27}\text{Cr}_{0.4}\text{H}_{1.75}$ [10], that includes several steps: (i) modelling of the hydride structure on the basis of hydrogen site solubility energy, $E_{\text{sol}}^{(i)}$ calculations; (ii) calculations of the distribution function for the site solubility energy; (iii) calculations of the activation energy for the most probable hydrogen diffusion pathways; (iv) estimation of hydrogen diffusion coefficient. Here we report on the results of the application of this approach to study bcc Ti-V-Cr alloys with low hydrogen concentration at the beginning of hydrogenation.

Method of Calculation

To simulate a disordered bcc Ti-V-Cr alloy we used a supercell constructed from $(4 \times 4 \times 2)$ -bcc unit cells and cut it along the $\langle 110 \rangle$ directions in such a manner as shown in Fig. 1(a). The final supercell consists of 32 metal atoms with random distribution of metallic atoms (we selected several representative configurations applying the Monte Carlo approach [11]). It can be considered as a good first-step approximation to study as both calculations done by applying Korringa-Kohn-Rostoker method within the coherent potential approximation (KKR-CPA) [12] and experiment [8] confirm that the $\text{Ti}_{0.33}\text{V}_{0.27}\text{Cr}_{0.4}$ alloy is completely disordered. To simulate hydrides a hydrogen atom was set in an interstitial tetrahedral (T) or octahedral (O) site that provides H/M ratio equal to 0.03125. Possible T-sites are shown in Fig. 1(a). All the energy characteristics of the alloy and hydride were calculated after the full structure relaxation that led to slight displacements of the atoms from their initial positions, see Fig. 1(b).

The calculation were done applying the plane-wave pseudo-potential density functional theory (PWP DFT) method using the Perdew–Burke–Ernzerhof generalized gradient approximations for exchange-correlation potential [13] and the ultrasoft Vanderbilt pseudopotentials as implemented in the Quantum Espresso package [14]. The kinetic energy cutoffs for wave functions and charge density expansion were taken 60 and 260 Ry, respectively. To save the computing time a total number of $3 \times 3 \times 3$ k -points in the irreducible Brillouin zone was used. Test calculations proved that increasing k -points up to $10 \times 10 \times 10$ did not affect dramatically the final results. Zero-point-energy (ZPE) contribution was taken into account within the framework of the linear-response method summing up zero-point vibrational energies of normal modes [15].

To determine hydrogen diffusion characteristics the formalism proposed in Ref. [3] was used. The activation energy E_a of hydrogen translational motion was determined using the nudged elastic band (NEB) method [16,17] as a barrier along the minimum energy path (MEP) between two hydrogen positions. The lattice parameters of the supercell were optimized all along the hydrogen displacement paths.

Results and Discussion

Following the previously developed algorithm for calculation of hydrogen diffusion in disordered alloys, first, we have to determine the preferable hydrogen site. It is to be noted that localization of hydrogen in bcc-Ti-V-Cr alloys is still questionable. According to calculation done applying the KKR-CPA the energy difference for hydrogen placed in tetrahedral (T) or octahedral (O) sites is negligible and the hydrogen site preference is affected by the calculation accuracy [7,9]. It can be explained by (i) neglecting the ZPE contribution that may play an important role in transition metal hydrides [18]; (ii) neglecting the local structure and difference in hydrogen-to-metal atom interaction (KKR-CPA considers “generalized” atoms in a geometrically ideal lattice, making no allowance for local distortions).

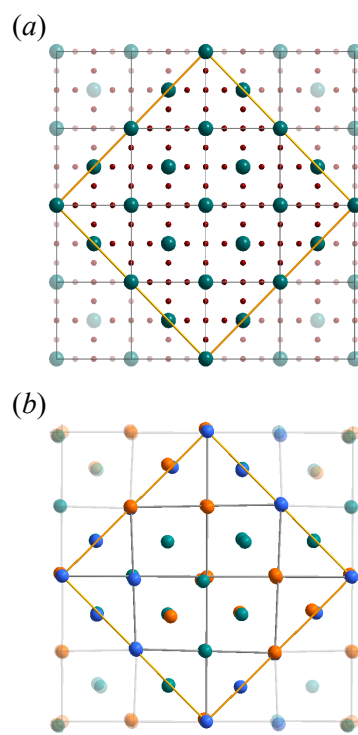


Fig. 1. (a) – top view of a supercell containing 32 metal atoms and 192 interstitial T-sites constructed from $(4 \times 4 \times 2)$ -bcc unit cells; large and small spheres represent metal and hydrogen atoms, respectively; (b) – top view of a selected configuration of the metal supercell after structural relaxation (orange, blue green correspond to Ti, V, Cr atoms, respectively).

In disordered ternary alloys such as Ti-V-Cr, neglecting local distortion due to the influence of the second coordination sphere, there are 15 different T- and 28 octahedral O-sites that we denote as $[\text{Ti}_{4-m-n}\text{V}_m\text{Cr}_n]$ (with m, n running from 0 to 4) and $[\text{Ti}_{6-m'-n'}\text{V}_{m'}\text{Cr}_{n'}]$ (with m', n' running from 0 to 6), respectively.

To estimate the hydrogen site preference, we calculated the hydrogen site solubility that is the energy that cost to remove a hydrogen atom from a given interstitial site of the supercell:

$$E_{\text{sol}}^i = E_{\text{tot}}^i(\text{hydride}) - [E_{\text{tot}}(\text{alloy}) + \frac{1}{2}E(\text{H}_2)], \quad (1)$$

where $E_{\text{tot}}(\text{alloy})$ and $E_{\text{tot}}^i(\text{hydride})$ are the total energy values for the alloy and hydride with one hydrogen atom placed in a certain interstitial site, $E(\text{H}_2)$ is the total energy of the H_2 molecule. $E(\text{H}_2)$ was calculated by placing an H_2 molecule in a $10 \times 10 \times 10 \text{ \AA}^3$ box and optimizing the distance between H atoms.

The supercell calculations prove that site stability is governed by local environment and that O-sites are, in general, unstable: only few of them were stabilized and exhibit solubility energy close to -0.52 eV , see Table 1, in other cases the hydrogen atom escapes O-sites stabilizing in a nearby T-site with the lowest energy. In Table 1 we also listed the average values of E_{sol}^i and metal-to-hydrogen distances obtained for hydrogen localized in T-sites. Here “average” means that the influence of the second coordination sphere is taken into account; if one supposes a normal distribution this is the expectation value, the standard deviation in this case is about 0.07 eV for E_{sol}^i and 0.005 \AA for $d_{\text{M-H}}$. It is to be noted that all the polyhedra are rather distorted and H is displaced towards Ti: in T-sites averaged Ti-H, V-H and Cr-H distances are equal to $1.24, 1.45$ and 1.90 \AA , respectively (for the non-distorted bcc structure with lattice parameter 2.981 \AA and hydrogen placed in T-site the metal-to-hydrogen distance is equal to 1.666 \AA).

For the O-sites, the metal-to-hydrogen distances are slightly longer, but the tendency remains the same: H is repelled by Cr and attracted by Ti. It is interesting to note that although H stabilized in O-sites is a rare case, once it happens, the solubility is better than average solubility in T-sites. Another point to pay attention is that the hydrogen solubility energy, and for O-sites in bcc lattice especially, is very sensitive to the second coordination sphere and to consider all the possibility is a laborious and not very beneficial task. Based on the selective calculations one can conclude that hydrogen may be stabilized in Ti-V-rich O-sites. But the geometrical aspect may play a key role.

Once the site solubility is calculated one can determine site occupancy using the Fermi-Dirac distribution for protons [19],

$$c^{(i)} = \frac{c \cdot P^{(i)}}{1 + \exp[(E_{\text{sol}}^{(i)} + f(c) - \mu)/RT]}, \quad (2)$$

where $c^{(i)}$ is the hydrogen occupation on site type i ; $c = \sum_i c^{(i)}$ is the total hydrogen site occupancy; $f(c)$ is the long-range effective H-H interaction, assumed to depend only on the total hydrogen concentration c [19]; $P^{(i)}$ is the probability to find a site type i for a given alloy composition; μ is the H-atom chemical potential in the metal; R and T are the gas constant and temperature, respectively. In our calculations H-H repulsive interaction is taken into account at the level of the Hamiltonian description. The probability to find a given T-site $[\text{Ti}_{4-m-n}\text{V}_m\text{Cr}_n]$ can be estimated as

$$P^{(i)} = \frac{4!}{(4-m-n)!m!n!} x^{(a-m-n)} y^m z^n. \quad (3)$$

The hydrogen site occupation at 294 K is listed in Table 1. As one can see the most occupied are sites $[\text{TiV}_2\text{Cr}]$ and $[\text{Ti}_2\text{VCr}]$.

Further, based on the formalism reported in our previous work [3] we applied NEB calculation to study hydrogen diffusivity. An example of such calculations for hydrogen motion inside a $[\text{Ti}_2\text{VCr}_3]$ octahedron from a $[\text{TiVCr}_2]$ T-site to an adjacent and an opposite $[\text{Ti}_2\text{VCr}]$ T-sites is

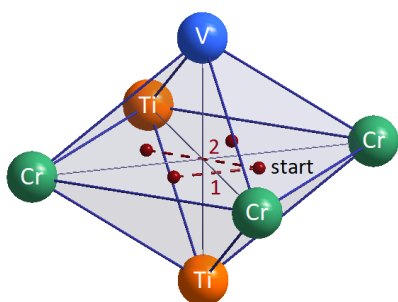
shown in Fig. 2. As one can see the calculated activation barriers are rather different: hydrogen jumps between adjacent T-sites are more favorable and diffusion path lies near the O-site avoiding it.

Table 1. Hydrogen site solubility energy and interatomic distances calculated for the stable interstitial sites in bcc hydride of $\text{Ti}_{0.33}\text{V}_{0.27}\text{Cr}_{0.4}$ with $\text{H}/\text{M} = 0.03125$. For T-sites the averaged values (over the sites with different second coordination sphere) are given. The T-site occupancy $c^{(i)}$ is given for $T = 294$ K.

Stable T-sites (averaged over site type)					
Site	$\langle E_{\text{sol}}^{(i)} \rangle$ (eV)	$\langle d_{\text{Ti-H}} \rangle$ (Å)	$\langle d_{\text{V-H}} \rangle$ (Å)	$\langle d_{\text{Cr-H}} \rangle$ (Å)	$c^{(i)}$
[Ti ₄]	-0.62	1.255	—	—	0.0001
[Ti ₃ V]	-0.58	1.240	1.535	—	0.0047
[Ti ₃ Cr]	-0.37	1.271	—	2.004	0.0016
[Ti ₂ V ₂]	-0.42	1.235	1.466	—	0.0053
[TiV ₃]	-0.39	1.192	1.455	—	0.0044
[Ti ₂ VCr]	-0.46	1.186	1.383	1.981	0.0177
[TiV ₂ Cr]	-0.33	1.247	1.515	1.963	0.0212
[Ti ₂ Cr ₂]	-0.39	1.221	—	1.843	0.0042
[V ₃ Cr]	-0.44	—	1.416	1.984	0.0012
[V ₄]	-0.42	—	1.478	—	0.0005
[TiVCr ₂]	-0.27	1.194	1.459	1.884	0.0030
[V ₂ Cr ₂]	-0.22	—	1.395	1.812	0.0033
[TiCr ₃]	-0.35	1.246	—	1.884	0.0002
[VCr ₃]	-0.12	—	1.334	1.814	0.0000
[Cr ₄]	-0.10	—	—	1.805	0.0000

Stabilized O-sites				
Site	$E_{\text{sol}}^{(i)}$ (eV)	$d_{\text{Ti-H}}$ (Å)	$d_{\text{V-H}}$ (Å)	$d_{\text{Cr-H}}$ (Å)
[TiV ₂ Cr ₃]	-0.485	1.4774	1.7796	1.9530
[Ti ₃ V ₂ Cr]	-0.549	1.4186	1.8265	2.1246
[TiV ₅]	-0.508	1.2847	1.6679	—
[Ti ₂ V ₃ Cr]	-0.528	1.3845	1.7146	1.9974
[Ti ₃ VCr ₂]	-0.528	1.4260	1.5846	1.8954

(a)



(b)

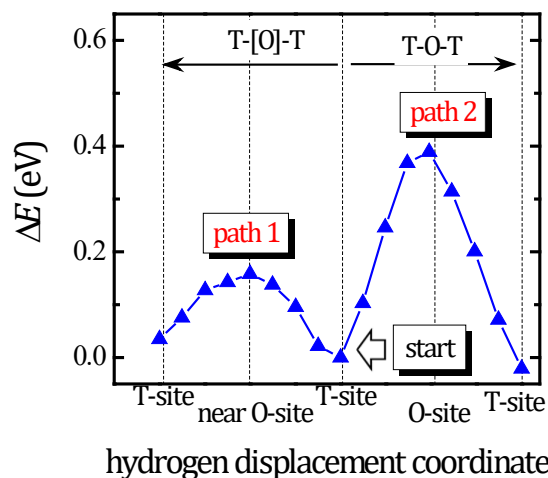


Fig. 2. Hydrogen diffusion pathways (a) and NEB energy profiles (b) for H motion inside the $[\text{Ti}_2\text{VCr}_3]$ octahedron from a $[\text{TiVCr}_2]$ T-site to an adjacent (path 1) and an opposite (path 2) $[\text{Ti}_2\text{VCr}]$ T-sites.

Accounting for ZPE contribution results to $E_a = 0.126$ eV. This value is close to the experimental one obtained for bcc $\text{Ti}_{0.11}\text{V}_{0.42}\text{Cr}_{0.47}\text{H}_{0.38}$ from ^1H nuclear magnetic resonance (NMR) relaxation measurements (0.11 eV) [20], but essentially lower than one determined from ^1H NMR self-diffusion experiment (0.20 eV) [4]. A possible issue of such a discrepancy between relaxation and diffusion measurements could be in inhomogeneity of the metallic atoms distribution in the studied sample (in relaxation measurements one probes the local jumps, whereas in diffusion experiments one studies long-range translational motion). In case of calculations one considers local jumps between two stable sites. Using the calculated E_a value we estimated the hydrogen diffusion coefficient using the approach reported earlier [3,10]:

$$D = nL^2\Gamma = nL^2 \frac{k_B T}{h} e^{-\frac{E_a}{k_B T}} = D_0 e^{-\frac{E_a}{k_B T}}. \quad (4)$$

Here L is the length of the diffusion jump, Γ is the frequency of jumps, k_B and T are the Boltzmann constant and temperature, respectively, n is a multiplier which depends on the geometry of the stable and transition states of the diffusing particle. For diffusion jumps in a bcc lattice between adjacent T-sites $n = 1$ and L is a half-length of the lattice parameter. Hence, finally one has for the diffusion coefficient at 294 K, $D = 1.9 \times 10^{-10} \text{ m}^2/\text{s}$ (with $D_0 = 2.7 \times 10^{-8} \text{ m}^2/\text{s}$) that is comparable with experimental data for bcc $\text{Ti}_{0.11}\text{V}_{0.42}\text{Cr}_{0.47}\text{H}_{0.38}$ [4].

Conclusions

DFT supercell calculations of the hydrogen site solubility in bcc disordered Ti-V-Cr alloys have revealed that hydrogen is mainly localized in tetrahedral sites formed by different metal species. However, all the polyhedra are rather distorted and hydrogen is displaced towards titanium. Both the hydrogen site stability and diffusion parameters (path length and activation energy) are especially sensitive to the second coordination sphere of the hydrogen atom, much more than obtained for fcc hydrides of Ti-V-Cr alloys [10]. The estimated values of the activation energy and hydrogen diffusion coefficient are in reasonable agreement with experimental data.

Acknowledgements

The calculations were carried out using computational facilities provided by Resource Center «Computer Center of SPbU» (<http://cc.spbu.ru/en>).

References

- [1] S. Miraglia, P. De Rango, S. Rivoirard, D. Fruchart, J. Charbonnier, N. Skryabina, Hydrogen sorption properties of compounds based on BCC $\text{Ti}_{1-x}\text{V}_x\text{Cr}_{1+x+y}$ alloys, *J. Alloys Compd.* 536 (2012) 1–6. doi:10.1016/j.jallcom.2012.05.008.
- [2] S. Nachev, P. De Rango, N. Skryabina, A. Skachkov, V. Aptukov, D. Fruchart, P. Marty, Mechanical behavior of highly reactive nanostructured MgH_2 , *Int. J. Hydrogen Energy.* 40 (2015) 17065–17074. doi:10.1016/j.ijhydene.2015.05.022.
- [3] K. Klyukin, M.G. Shelyapina, D. Fruchart, DFT calculations of hydrogen diffusion and phase transformations in magnesium, *J. Alloys Compd.* 644 (2015) 371–377. doi:10.1016/j.jallcom.2015.05.039.
- [4] A.V. Vyvodtceva, M.G. Shelyapina, A.F. Privalov, Y.S. Chernyshev, D. Fruchart, ^1H NMR study of hydrogen self-diffusion in ternary Ti-V-Cr alloys, *J. Alloys Compd.* 614 (2014) 364–367. doi:10.1016/j.jallcom.2014.06.023.

-
- [5] J. Völkl, G. Alefeld, Diffusion of hydrogen in metals, in: G. Alefeld, J. Völkl (Eds.), *Hydrog. Met. I Basic Prop.*, Springer Berlin Heidelberg, Berlin, Heidelberg, 1978: pp. 321–348. doi:10.1007/3540087052_51.
- [6] H. Wipf, Diffusion of hydrogen in metals, in: H. Wipf (Ed.), *Hydrog. Met. III Prop. Appl.*, Springer Berlin Heidelberg, Berlin, Heidelberg, 1997: pp. 51–91. doi:10.1007/BFb0103401.
- [7] M.G. Shelyapina, A. V. Vyvadtceva, K.A. Klyukin, O.O. Bavrina, Y.S. Chernyshev, A.F. Privalov, D. Fruchart, Hydrogen diffusion in metal-hydrogen systems via NMR and DFT, *Int. J. Hydrogen Energy*. 40 (2015) 17038–17050. doi:10.1016/j.ijhydene.2015.05.176.
- [8] S. Miraglia, D. Fruchart, N. Skryabina, M. Shelyapina, B. Ouladiaf, E.K. Hlil, P. de Rango, J. Charbonnier, Hydrogen-induced structural transformation in $\text{TiV}_{0.8}\text{Cr}_{1.2}$ studied by in situ neutron diffraction, *J. Alloys Compd.* 442 (2007) 49–54. doi:10.1016/j.jallcom.2006.10.168.
- [9] M.G. Shelyapina, V.S. Kasperovich, N.E. Skryabina, D. Fruchart, Ab initio calculations of the stability of disordered Ti-V-Cr solid solutions and their hydrides, *Phys. Solid State*. 49 (2007) 399–402. doi:10.1134/S1063783407030018.
- [10] O.O. Bavrina, M.G. Shelyapina, K.A. Klyukin, D. Fruchart, First-principle modelling of hydrogen site solubility and diffusion in disordered Ti-V-Cr alloys, *Int. J. Hydrogen Energy*. (2018) doi:10.1016/j.ijhydene.2018.07.128.
- [11] K. Binder, Ordering of the face-centered-cubic lattice with nearest-neighbor interaction, *Phys. Rev. Lett.* 45 (1980) 811–814.
- [12] M.G. Shelyapina, D. Fruchart, P. De Rango, J. Charbonnier, S. Rivoirard, N. Skryabina, S. Miraglia, E.K. Hlil, P. Wolfers, First-principles investigation of the stability of the Ti-V-Cr ternary alloys and their related hydrides, *AIP Conf. Proc.* 837 (2006) 104–111. doi:10.1063/1.2213065.
- [13] J.P. Perdew, K. Burke, M. Ernzerhof, Generalized gradient approximation made simple, *Phys. Rev. Lett.* 77 (1996) 3865–3868. doi:10.1103/PhysRevLett.77.3865.
- [14] P. Giannozzi, S. Baroni, N. Bonini, M. Calandra, R. Car, C. Cavazzoni, D. Ceresoli, G.L. Chiarotti, M. Cococcioni, I. Dabo, A. Dal Corso, S. De Gironcoli, S. Fabris, G. Fratesi, R. Gebauer, U. Gerstmann, C. Gougoussis, A. Kokalj, M. Lazzeri, L. Martin-Samos, N. Marzari, F. Mauri, R. Mazzarello, S. Paolini, A. Pasquarello, L. Paulatto, C. Sbraccia, S. Scandolo, G. Sclauzero, A.P. Seitsonen, A. Smogunov, P. Umari, R.M. Wentzcovitch, QUANTUM ESPRESSO: A modular and open-source software project for quantum simulations of materials, *J. Phys. Condens. Matter*. 21 (2009) 395502-1–19. doi:10.1088/0953-8984/21/39/395502.
- [15] S. Baroni, P. Giannozzi, A. Testa, Green's-function approach to linear response in solids, *Phys. Rev. Lett.* 58 (1987) 1861–1864. doi:10.1103/PhysRevLett.58.1861.
- [16] H. Jonsson, G. Mills, K.W. Jacobsen, Classical and quantum dynamics in condensed phase simulations, in: B.J. Berne, G. Ciccotti, D.F. Coker (Eds.), *Nudged Elastic Band Method Find. Minim. Energy Paths Transitions*, World Scientific Publishing, Singapore, 1998: pp. 385–404.
- [17] G. Henkelman, H. Jónsson, P. Giannozzi, S. Baroni, N. Bonini, M. Calandra, R. Car, C. Cavazzoni, D. Ceresoli, G.L. Chiarotti, M. Cococcioni, I. Dabo, A. Dal Corso, S. De Gironcoli, S. Fabris, G. Fratesi, R. Gebauer, U. Gerstmann, C. Gougoussis, A. Kokalj, M. Lazzeri, L. Martin-Samos, N. Marzari, F. Mauri, R. Mazzarello, S. Paolini, A. Pasquarello, L. Paulatto, C. Sbraccia, S. Scandolo, G. Sclauzero, A.P. Seitsonen, A. Smogunov, P. Umari, R.M. Wentzcovitch, Improved tangent estimate in the nudged elastic band method for finding minimum energy paths and saddle points, *J. Phys. Condens. Matter*. 21 (2000) 395502-1–19. doi:10.1063/1.1323224.

-
- [18] T.J. Frankcombe, The importance of vibrations in modelling complex metal hydrides, *J. Alloys Compd.* 446–447 (2007) 455–458. doi:10.1016/j.jallcom.2007.01.050.
- [19] R.C. Brouwer, R. Griessen, Heat of solution and site energies of hydrogen in disordered transition-metal alloys, *Phys. Rev. B.* 40 (1989) 1481–1494. doi:10.1103/PhysRevB.40.1481.
- [20] V.S. Kasperovich, M.G. Shelyapina, B. Khar’Kov, I. Rykov, V. Osipov, E. Kurenkova, A. V. Ievlev, N.E. Skryabina, D. Fruchart, S. Miraglia, P. De Rango, NMR study of metal-hydrogen systems for hydrogen storage, *J. Alloys Compd.* 509 (2011) S804–S808. doi:10.1016/j.jallcom.2010.10.195.